IEEE Access
Multidisciplinary | Rapid Review | Open Access Journal

Received March 29, 2022, accepted April 29, 2022, date of publication May 3, 2022, date of current version May 11, 2022.

Digital Object Identifier 10.1109/ACCESS.2022.3172505

Calibration Method for Industrial Robots Based on the Principle of Perigon Error Close

XIRUI LI, ENZHENG ZHANG, XIUJUN FANG, AND BIN ZHAI
Faculty of Mechanical Engineering and Automation, Zhejiang Sci-Tech University, Hangzhou 310018, China
Corresponding author: Enzheng Zhang (zhangez@zstu.edu.cn)

This work was supported by the National Natural Science Foundation of China under Grant 52175489.

ABSTRACT For the problem that the self-error of industrial robot calibration device has influence on calibration accuracy, a calibration method of industrial robots based on the principle of Perigon Error Close is proposed. In the method, the theory that the sum of circular indexing interval errors around a circle is zero is applied to robot calibration to improve robot calibration accuracy. The calibration principle of the proposed method is provided in detail and the calibration equation is derived in this paper. The calibration system based on the proposed method was constructed with one semiconductor laser and two position sensing detectors (PSDs) fixed on a rotary table. Based on the position error data obtained from laser spot position on the PSDs, the robot kinematics parameter errors were identified by using Levenberg Marquardt (LM) algorithm. The robot calibration experimental setup was constructed and the related verification experiments were carried out. The model parameter identification experiment validates the feasibility of the proposed method for industrial robot calibration. The calibration compensation experiment results of industrial robots show that the maximum position error of the robot is reduced by 71.9% and the average position error is reduced by 77.8%, which validates the effectiveness of the proposed method for industrial robot calibration.

INDEX TERMS Calibration, industrial robots, principle of Perigon error close, laser, PSD.

I. INTRODUCTION

Industrial robots are widely used in various fields for the advantages of high repeatable positioning accuracy, high reliability and strong adaptability [1], [2]. In practical application, the long-term and high-intensity use of the robot could cause great wear and tear on the robot joints, which would make the actual model parameters of the robot deviate from the theoretical values and lead to the decline of positioning accuracy. Therefore, the timely calibration of robot is quite necessary and is the key to guaranteeing its working accuracy [3]–[6].

The basic principle of robot calibration is to identify the model parameter errors by using the measured end-pose data of the robot, and then compensate the robot model to improve its positioning accuracy [7]–[11]. The high measurement accuracy of laser tracker makes it an important equipment for precision robot calibration applications, while the high cost makes it difficult to be widely used [12]–[15].

Therefore, researchers have carried out a lot of studies on robot calibration methods, among which the calibration methods of imposing constraints on end-effector can be roughly divided into two types: contact and non-contact calibration methods [16]–[18]. The contact calibration methods generally require external reference measurement component to complete the calibration [19].

For example, Shi *et al.* [20] constructed a geometric point constraint calibration system by using a sampling needle installed on the robot end-effector and a sampling box used for placing the crop seeds, which improved the positioning accuracy of robot. He *et al.* [21] constructed a multi-position constraint system by using two standard devices and a non-bar device to improve the accuracy of robot. Joubair *et al.* [22] constructed a distance and sphere constraint calibration system with a precision touch probe installed on the robot end-effector and a special triangular plate with three datum spheres, which improved the accuracy of the robot in a specific workspace.

The problem existed among the above calibration methods is that the contact error during calibration has influence on the accuracy of the measurement data, which would affect the calibration accuracy. Comparing with contact calibration methods, non-contact calibration methods do not require physical contact, which can effectively avoid the influence

The associate editor coordinating the review of this manuscript and approving it for publication was Bidyadhar Subudhi.

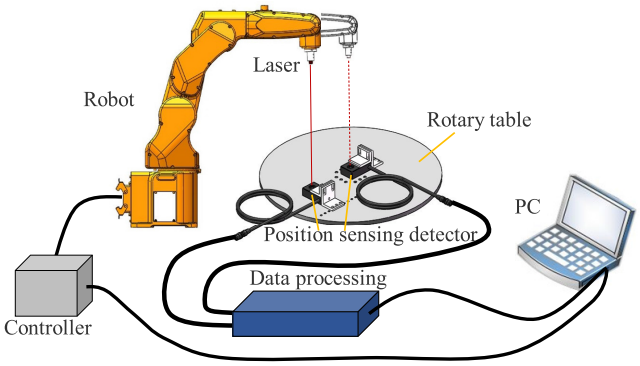

FIGURE 1. Calibration system of industrial robots based on principle of perigon error close.

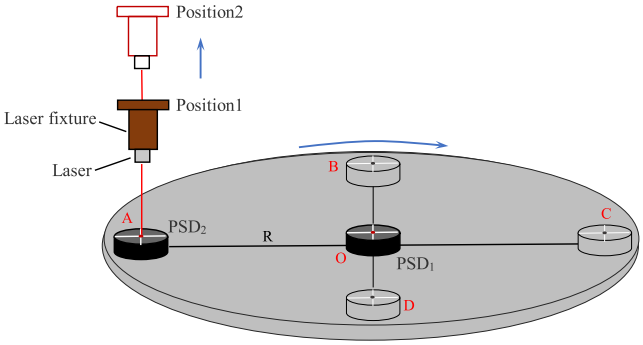

FIGURE 2. Principle of perigon error close constraint.

of contact errors on the calibration accuracy [23], [24]. Gao *et al.* [25] proposed a calibration method by using a laser pointer installed on the robot end-effector and a position sensing detector (PSD) arbitrarily placed in the work space, and established the optimization model for calibration by imposing virtual point constraint on the laser beam. However, this method only considers the joint offset errors of the robot, and does not consider other parameter errors. Du *et al.* [26] constructed a calibration system by using a laser pointer, a rotatable PSD and fixed cameras, and applied virtual sphere constraint to the laser beam for calibration to improve the positioning accuracy of robot. Guo *et al.* [27] used one single laser displacement sensor (LDS) and one master sphere installed on the robot end-effector to construct the calibration system, and calibrated the kinematic parameters by imposing spherical center point constraint on the laser beam, which improved the calibration accuracy and efficiency of the robot.

Summering the above calibration methods with constraint imposed on the robot end-effector, they can improve the accuracy of robot to varying degrees, however, the common problem among these methods is that the self-error of robot calibration device could have influence on calibration accuracy. Therefore, this paper proposes a calibration method of industrial robots based on the principle of Perigon Error Close. The definition of the Perigon Error Close [28] is that the sum of circular indexing interval errors around a circle is zero, and the Perigon Error Close is applied to robot calibration to improve robot calibration accuracy.

The rest of the paper is organized as follows: In section II, the calibration system of the proposed method is introduced. In section III, the calibration principle of the proposed method is provided in detail and the calibration equations are derived. In section IV, three verification experiments and the corresponding experimental results are illustrated. Finally, the conclusion is presented in Section V.

II. CALIBRATION SYSTEM

The calibration system for industrial robot based on the principle of Perigon Error Close is shown in Figure 1. The calibration system include laser, rotary table, two PSDs, data processing module and PC software. Firstly, the laser is installed on the end-effector of the robot, and the axis direction of the laser is required to be the same as the axis direction of the end-effector. Two PSDs are fixed on the rotary table of the calibration system, one PSD is fixed at the center of the rotary table and another PSD is fixed on the circle with a radius of R. Secondly, the laser beam need to vertically incident onto the photosensitive surface of the two PSDs, respectively, the spot positions of the laser beam on the two PSDs are obtained through the data processing module and transmitted to the PC software, then, the position coordinates of the spot on the photosensitive surface of the PSDs are obtained. Thirdly, the PC software is used to control the rotary table to rotate to different target positions, and the data required for calibration are obtained by using the same data acquisition process above. The calibration method of industrial robots based on the principle of Perigon Error Close proposed in this paper is used to identify the model parameters of the robot, and the errors of the identified model parameters are compensated to the kinematic model of the robot, and then the calibration of the industrial robot is completed.

III. CALIBRATION METHOD

The principle of the proposed calibration method in this paper is shown in Figure 2. According to the joint structure of the industrial robot to be calibrated, the theoretical transformation matrix ${}^{j}T_{j+1}$ of the joint coordinate system between two adjacent joints can be derived by

$$ {}^{j}T_{j+1} = \begin{bmatrix} \cos\theta_j & -\cos\alpha_j \sin\theta_j & \sin\alpha_j \sin\theta_j & a_j \cos\theta_j \\ \sin\theta_j & \cos\alpha_j \cos\theta_j & -\sin\alpha_j \cos\theta_j & a_i \sin\theta_j \\ 0 & \sin\alpha_j & \cos\alpha_j & d_j \\ 0 & 0 & 0 & 1 \end{bmatrix} \tag{1} $$

where, $j+1$ is the joint number, $j = 0, 1, 2, 3, 4, 5$. a_j, α_j, θ_j, d_j are the link length, link twist, joint angle, link offset, respectively.

The theoretical transformation matrix T of the robot end coordinate system relative to the base coordinate system can be obtained by multiplying the six joint

transformation matrices

$$T = {}^0T_1\,{}^1T_2\,{}^2T_3\,{}^3T_4\,{}^4T_5\,{}^5T_6 = \begin{bmatrix} n_x & o_x & a_x & p_x \\ n_y & o_y & a_y & p_y \\ n_z & o_z & a_z & p_z \\ 0 & 0 & 0 & 1 \end{bmatrix} \quad (2)$$

where, (p_x, p_y, p_z) is the position coordinate of the robot end coordinate system relative to the base coordinate system. The matrix composed of (n_x, n_y, n_z), (o_x, o_y, o_z) and (a_x, a_y, a_z) is the direction cosine of the three unit vectors.

Suppose that the joint angle data of the industrial robot is $(\theta_1, \theta_2, \theta_3, \theta_4, \theta_5, \theta_6)$, by substituting the joint angle data into formula (2), then the end pose data $(p_x, p_y, p_z, \alpha, \beta, \gamma)$ of the robot can be obtained. In the calibration system shown in Figure 1, the axis direction of the laser is the same as that of the end-effector, and according to the principle of Perigon Error Close constraint shown in Figure 2, the position coordinate conversion equation from the end position coordinate of the robot to the center of laser spot on the PSD can be derived by

$$\frac{x - p_x}{a_x} = \frac{y - p_y}{a_y} = \frac{z - p_z}{a_z} \quad (3)$$

where, (x, y, z) is the position coordinate of the laser spot center on the PSD.

Suppose that the nominal position coordinate of laser spot center on the PSD obtained by equation (3) is $\mathrm{P}_{ik}(X_{ik}, Y_{ik}, Z_{ik})$, where, i is the number of data, and i is taken as 1,2, k is the position of the PSD, and k is taken as O, A, B, C and D. As is shown in Figure 2, the measurement steps are as follows: Firstly, when the PSD_2 is at position A, the laser beam is adjusted to be vertically incident onto the photosensitive surface of PSD_2, and the laser beam is positioned to the spot center of the photosensitive surface through the data processing module. At the same time, the robot is controlled to move to position 1, and a set of robot joint angle data is collected by using the robot controller, thus the end pose data is obtained through the forward kinematics of the robot.

Secondly, the robot is controlled to move from position 1 to position 2 along the axis direction, and when the robot is at position 2, the other end pose data can be obtained in the same way. Thirdly, the end pose data of the two positions are substituted into equation (3) to establish a system of equations, and the nominal value of $\mathrm{P}_A(X_A, Y_A, Z_A)$ can be obtained by solving the system of equations. Fourthly, by using the same measurement method as getting the nominal position coordinate P_A, the nominal position coordinate $\mathrm{P}_O(X_O, Y_O, Z_O)$ of the laser spot center on the PSD_1 can be obtained. Fifthly, the rotary table is controlled by PC software to rotate to the positions of B, C and D in sequence, and the nominal position coordinate of laser spot center on the PSD_2 at each position are obtained through the same measurement method, respectively, thus the nominal values corresponding to the three positions of B, C and D are expressed as P_B, P_C, and P_D, respectively. Finally, all the measurement data of the five position points are used for robot model parameter identification.

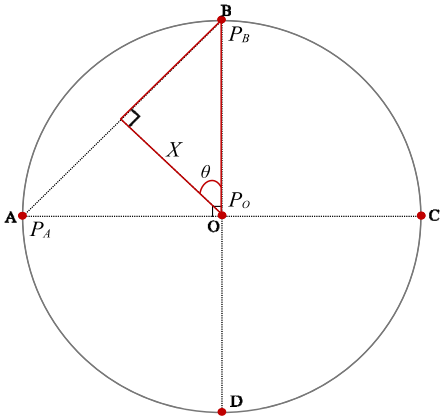

FIGURE 3. Circular indexing angle measurement principle.

Suppose that the actual position coordinate of laser spot center on PSD under the robot base coordinate system is $p_k(x_k, y_k, z_k)$. Due to the errors of robot kinematics parameter, the nominal position of the laser spot center on the PSD is deviated from the actual position, and its position deviation Δe_k can be derived by

$$\Delta e_k = p_k - \mathrm{P}_k = J_k \Delta\delta' \quad (4)$$

where, P_k is the nominal value. k is taken as O, A, B, C and D. P_O is the nominal value of laser spot center on the PSD_1 when PSD_1 is at position O. P_A, P_B, P_C, P_D are the nominal values of laser spot center on the PSD_2 when PSD_2 is at four positions A, B, C and D, respectively. J_k is the Jacobian matrix. $\Delta\delta'$ are the kinematic parameter errors.

In the proposed calibration method, as is shown in Figure 2, the four target positions of PSD_2 on the rotary table are at the four equipartition points of a circle, respectively, and the actual position coordinate $p_k(x_k, y_k, z_k)$ under the robot base coordinate system can be obtained by equation (4). As is shown in Figure 3, according to the principle of similar triangles, the distance X from the point O to the line segment AB can be derived by

$$\frac{p_B - p_O}{p_B - p_A} = \frac{X}{p_A - p_O} \quad (5)$$

The distance X can be obtained from equation (5), and then according to the properties of the right triangle, the angle θ can be expressed by

$$\theta = \arctan\frac{(p_B - p_A)/2}{X} = \arctan\frac{(p_B - p_A)^2}{2(p_B - p_O)\cdot(p_A - p_O)} \quad (6)$$

According to the circular indexing angle measurement principle shown in Figure 3, the circular indexing interval error of PSD_2 between the two adjacent positions of A and B can be derived by

$$\mu_{AOB} = \frac{\pi}{2} - 2\theta = \frac{\pi}{2} - 2\arctan\frac{(p_B - p_A)^2}{2(p_B - p_O)\cdot(p_A - p_O)} \quad (7)$$

Through the same circular indexing interval error obtaining principle, the other three circular indexing interval errors can be obtained. And based on the theory that the sum of circular indexing interval errors around a circle is zero, then the sum of the obtained four circular indexing interval errors can be expressed by

$$\mu_{AOB} + \mu_{BOC} + \mu_{COD} + \mu_{DOA} = 0 \tag{8}$$

The kinematic calibration equation based on the principle of Perigon Error Close can be obtained by substituting equation (4) and equation (7) into equation (8)

$$G \cdot \Delta\delta' = H \tag{9}$$

where, G and H are calibration equation parameters, and the G and H can be derived by (10) and (11), as shown at the bottom of the page.

The kinematic calibration equation (9) can be used to identify the parameters of the robot model. In order to improve the robustness and accuracy of parameter identification, the analytical method is used to analyze and eliminate the redundant parameters in the robot model, and the model parameter errors after processing can be expressed as

$$\begin{aligned}\Delta\delta = (&\Delta a_1 \ldots \Delta a_6, \Delta\alpha_1 \ldots \Delta\alpha_3, \Delta\theta_1 \ldots \Delta\theta_3, \Delta d_1 \ , \\ &\Delta d_3 \ldots \Delta d_6)^T\end{aligned} \tag{12}$$

where, Δa_i, $\Delta\alpha_i$, $\Delta\theta_i$, Δd_i are the link length errors, link twist errors, joint angle errors, link offset errors, respectively.

In order to improve the accuracy of robot model parameter identification, the robot kinematics parameter errors identification is carried out by LM algorithm, and the robot kinematics parameter errors can be derived by

$$\Delta\delta_{n+1} = \left(G_n^T \cdot G_n + \lambda I\right)^{-1} \cdot G_n^T \cdot H_n, n = 0, 1, 2, \ldots, N \tag{13}$$

where, λ is the damping coefficient. n is the number of iterations. G_n, H_n are the calibration equation parameters of iteration.

The identification of model parameters based on LM algorithm can be iterated by equation (13), in which the initial values of the iterative identification parameter are the theoretical kinematics model parameters δ_0, and the iterative identification equation of robot kinematics model parameters δ can be derived by

$$\delta_{n+1} = \delta_n + \Delta\delta_{n+1}, \quad n = 0, 1, 2, \ldots, N \tag{14}$$

Substituting the robot joint angle data and the theoretical position coordinate data of the laser spot center on PSDs into equation (14) for iteration, during the iteration process, when the $\Delta\delta$ is less than the preset threshold, iterative process ends, then the model parameter errors and robot kinematics model parameters δ_N can be obtained.

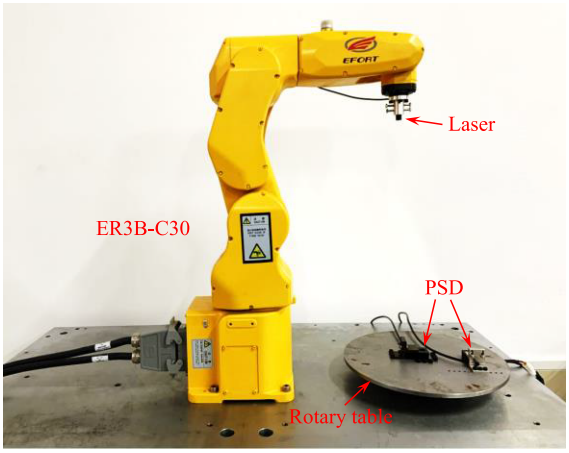

FIGURE 4. Experimental setup.

IV. EXPERIMENTAL RESULTS

In order to verify the feasibility and effectiveness of the proposed robot calibration method, three experiments were performed, including simulation experiment of model parameter identification, calibration compensation experiment and comparison experiment of calibration methods.

An experimental setup for industrial robot calibration based on the principle of Perigon Error Close was constructed, as is shown in Figure 4. The industrial robot to be calibrated is ER3B-C30, of which the repeated positioning

$$G = \begin{bmatrix} 2\left[(P_B - P_O)(J_A - J_O) + (P_A - P_O)(J_B - J_O) - (P_B - P_A)(J_B - J_A)\right] \\ 2\left[(P_C - P_O)(J_B - J_O) + (P_B - P_O)(J_C - J_O) - (P_C - P_B)(J_C - J_B)\right] \\ 2\left[(P_D - P_O)(J_C - J_O) + (P_C - P_O)(J_D - J_O) - (P_D - P_C)(J_D - J_C)\right] \\ 2\left[(P_D - P_O)(J_A - J_O) + (P_A - P_O)(J_D - J_O) - (P_D - P_A)(J_D - J_A)\right] \end{bmatrix} \tag{10}$$

$$H = \begin{bmatrix} (P_B - P_A)^2 - 2(P_B - P_O)(P_A - P_O) \\ (P_C - P_B)^2 - 2(P_C - P_O)(P_B - P_O) \\ (P_D - P_C)^2 - 2(P_D - P_O)(P_C - P_O) \\ (P_D - P_A)^2 - 2(P_D - P_O)(P_A - P_O) \end{bmatrix} \tag{11}$$

accuracy is 0.02 mm. The laser X650N5 used in the setup is a semiconductor laser, whose spot diameter of the output laser is 0.5 mm, the output power is 5 mw, and the laser wavelength is 650 nm. The two PSDs in the experimental setup are Thorlabs PDP90A lateral effect position sensors, whose detecting wavelength range is 320 to 1100 nm and effective detection aperture is 9 mm, and the measurement accuracy of PSDs is 0.75 μm. The two PSDs are fixed on a round plate made of invar material, and the round plate can rotate with the rotary table.

A. SIMULATION EXPERIMENT OF MODEL PARAMETER IDENTIFICATION

In order to verify the feasibility of the proposed calibration method for robot model parameter identification, the simulation experiment is carried out based on MATLAB. In the simulation experiment, 10 sets of measurement data are obtained at five positions of PSDs by using the measurement method in Section III, and 50 sets of measurement data are substituted into the kinematic calibration equation for model parameter identification. Firstly, the robot model is built with the theoretical kinematics model parameters of ER3B-C30. The target sampling points are planned in joint space of the robot, and the end pose data of robot are obtained through forward solution. Secondly, the preset parameter errors as shown in the fourth column of Table 1 are added to the parameters of the kinematic model of the robot, and the new robot end pose data are obtained through the forward solution. Thirdly, the proposed calibration method is used to identify the model parameter errors based on the above two sets of pose data. The simulation experiment results of model parameter identification are shown in Table 1.

As is shown in Table 1, the simulation experiment results indicate that the identified maximum link length deviation of each joint is 0.051 mm, the maximum link twist deviation of each joint is 0.009°, the maximum link offset deviation of each joint is 0.065 mm, and the maximum joint angle deviation of each joint is 0.006°. The experimental results demonstrate that all the identified model parameter errors are in good agreement with the preset errors, respectively. The results of robot position errors before and after calibration are shown in Figure 5.

The experimental results show that the position errors of the robot after calibration are smaller than the position errors before calibration, which verifies the feasibility of the proposed method for robot model parameter identification.

B. CALIBRATION COMPENSATION EXPERIMENT

In order to verify the effectiveness of the proposed calibration method for industrial robot model parameter identification, the calibration compensation experiment is performed with the setup shown in Figure 4. In the experiment, AT960 laser tracker is used to measure the actual position data of the robot end so as to obtain the position errors of the robot. The specific steps of the experiment are as follows: Firstly, 50 target sampling points are planned in the robot work space, and the robot is controlled to move to the target sampling points, at the same time, the position data of each point is measured with the laser tracker. Secondly, the proposed calibration method is used to identify the model parameters of the robot, and then the identified new model parameters are used to replace the original parameters of the robot, so as to compensate the robot model parameters. Thirdly, the robot is controlled to move to the 50 target sampling points again, and the laser tracker is used to simultaneously measure the position data of each point. Finally, the position errors before and after calibration compensation are compared to verify the effectiveness of the proposed method.

TABLE 1. Simulation experiment results.

Joint number	Kinematic parameters	Initial values	Preset errors	Identified errors
Joint 1	a_1 (mm)	0	0.2	0.247
	α_1 (°)	90	0.03	0.039
	d_1 (mm)	367.5	0.5	0.563
	θ_1 (°)	0	0.04	0.042
Joint 2	a_2 (mm)	295	0.2	0.199
	α_2 (°)	0	-0.05	-0.051
	d_2 (mm)*	0	*	*
	θ_2 (°)	90	0.02	0.019
Joint 3	a_3 (mm)	37	0.1	0.142
	α_3 (°)	90	0.04	0.048
	d_3 (mm)	0	0.5	0.565
	θ_3 (°)	0	0.07	0.076
Joint 4	a_4 (mm)	0	-0.2	-0.203
	α_4 (°)*	90	*	*
	d_4 (mm)	295.5	0.3	0.338
	θ_4 (°)*	0	*	*
Joint 5	a_5 (mm)	0	-0.6	-0.651
	α_5 (°)*	-90	*	*
	d_5 (mm)	0	-0.5	-0.561
	θ_5 (°)*	90	*	*
Joint 6	a_6 (mm)	0	0.2	0.202
	α_6 (°)*	0	*	*
	d_6 (mm)	78.5	0.2	0.262
	θ_6 (°)*	0	*	*

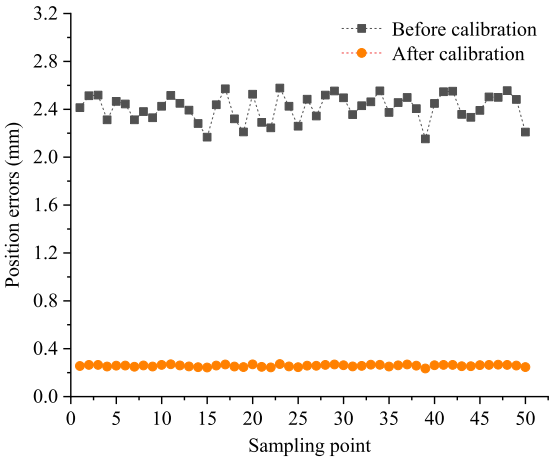

FIGURE 5. Simulation experiment results before and after calibration.

TABLE 2. Identified kinematics parameters.

Joint	a (mm)	α (°)	d (mm)	θ (°)
1	0.196	89.897	367.500	-0.304
2	295.386	0.066	0	90.614
3	36.973	89.857	-0.004	-0.188
4	-0.027	90	295.698	0
5	0.196	-90	0.004	90
6	0.196	0	78.528	0

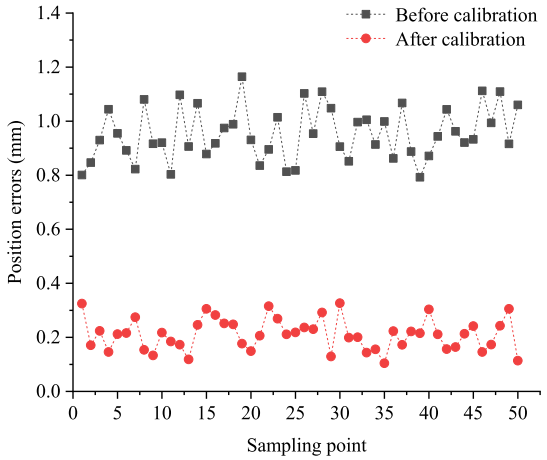

FIGURE 6. Experimental results before and after calibration.

TABLE 3. Kinematics parameters.

Joint	a (mm)	α (°)	d (mm)	θ (°)
1	0	90	367.5	0
2	295	0	0	90
3	37	90	0	0
4	0	90	295.5	0
5	0	-90	0	90
6	0	0	78.5	0

The actual model parameters of the robot identified by the proposed calibration method are shown in Table 2, and the comparison experimental results of robot position errors before and after calibration are shown in Figure 6.

The experimental results indicate that the maximum position error of the robot is reduced from 1.164 mm to 0.326 mm after calibration, and the average position error is reduced from 0.953 mm to 0.211 mm after calibration compensation. The calibration compensation experiment results demonstrate that the proposed calibration method effectively reduces position errors of the robot, which verifies the effectiveness of the proposed method for robot calibration.

C. COMPARISON EXPERIMENT OF CALIBRATION METHODS

In this experiment, the robot calibration method based on geometric radius constraint and the proposed calibration method are used for robot calibration, respectively, so as to compare the calibration compensation performance between them.

TABLE 4. Identified kinematics parameters based on the principle of perigon error close.

Joint	a (mm)	α (°)	d (mm)	θ (°)
1	0.310	90.481	367.500	-0.475
2	295.676	-0.206	0	90.759
3	36.957	90.381	0.001	-0.279
4	-0.043	90	295.814	0
5	0.311	-90	-0.001	90
6	0.311	0	78.501	0

TABLE 5. Identified kinematics parameters based on the geometric.

Joint	a (mm)	α (°)	d (mm)	θ (°)
1	0.554	90.293	367.500	-0.430
2	296.206	-0.416	0	90.957
3	36.924	90.155	-0.002	-0.712
4	-0.075	90	296.073	0
5	0.555	-90	0.001	90
6	0.557	0	78.511	0

TABLE 6. Position errors before and after calibration.

Position errors(mm)	Before calibration	Geometric radius constraint	Principle of Perigon Error Close
Average	0.953	0.299	0.218
Max	1.164	0.439	0.337

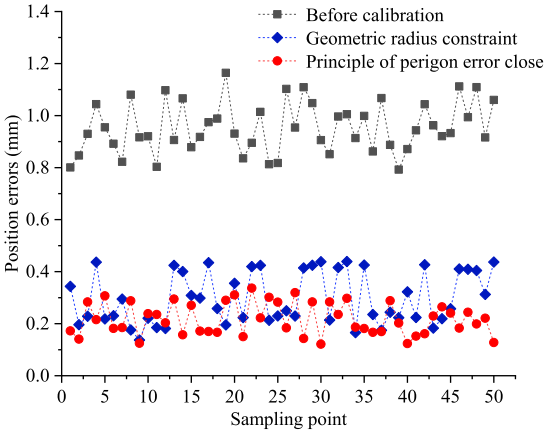

FIGURE 7. Comparison experimental results of calibration methods.

The kinematic parameters of the robot based two methods are shown in Table 3. Firstly, 50 sets of experimental measurement data are re-collected by using the measurement method in Section III. Secondly, the robot calibration method based on geometric radius constraint is used to identify and compensate the model parameters of the robot by using the same experimental steps in Section B. Thirdly, the robot is controlled to move to the 50 target sampling points again, and the laser tracker is used to simultaneously measure the position data of each point, so as to obtain the position errors data before and after calibration compensation based on this method.

The actual model parameters of the robot identified by the proposed calibration method and geometric radius constraint method are shown in Table 4 and Table 5, and the comparison experimental results are shown in Table 6 and Figure 7.

The experimental results indicate that the average position error of the calibration method based on geometric radius constraint is 0.299 mm, and that of the proposed calibration method is 0.218 mm. The experimental results demonstrate that both calibration methods can effectively reduce the position errors of the robot. Comparing with the robot calibration method based on geometric radius constraint, the proposed calibration method has better performance in reducing the position errors of robot.

V. CONCLUSION

In this paper, a calibration method for industrial robots based on the principle of Perigon Error Close is proposed. The principle of Perigon Error Close used in robot calibration was described in detail, and the corresponding robot calibration experimental setup was designed and constructed. The simulation experiment was performed, which verifies the feasibility of the proposed method for robot model parameter identification. In the calibration compensation experiment for ER3B-C30 robot, after calibration compensation, the maximum position error of the robot was reduced from 1.164 mm to 0.326 mm, and the average position error was reduced from 0.953 mm to 0.211 mm. In the comparison experiment, compared with the calibration method based on geometric radius constraint, the robot average position error was reduced by 0.08 mm by using the proposed calibration method. All these experimental results verify the feasibility and effectiveness of the proposed calibration method used in robot model parameter identification and compensation.

Considering the harsh working circumstances with proposed calibration system in the future, some measures should be taken to solve the problems of installation error and laser drift and to further improve calibration accuracy, which are our important work in the future.

REFERENCES

[1] Y. Tong, Y. Huang, L. Yang, C. Li, and X. Zhang, "Experiment study of positioning accuracy for a SCARA robot," in *Mechanism and Machine Science*. Singapore: Springer, 2017, pp. 317–324.

[2] Z. B. Li, S. Li, and X. Luo, "An overview of calibration technology of industrial robots," *IEEE/CAA J. Autom. Sinica*, vol. 8, no. 1, pp. 27–40, Jan. 2021.

[3] Y. Jiang, L. Yu, H. Jia, H. Zhao, and H. Xia, "Absolute positioning accuracy improvement in an industrial robot," *Sensors*, vol. 20, no. 16, p. 4354, Aug. 2020.

[4] M. Franaszek, G. S. Cheok, and J. A. Marvel, "Reducing localization error of vision-guided industrial robots," in *Proc. IEEE Int. Symp. Robot. Sensors Environ. (ROSE)*, Jun. 2019, pp. 183–189.

[5] T. Kubela, A. Pochyly, and V. Singule, "Investigation of position accuracy of industrial robots and online methods for accuracy improvement in machining processes," in *Proc. Int. Conf. Electr. Drives Power Electron. (EDPE)*, Sep. 2015, pp. 385–388.

[6] Z. Liu, Q. Wang, and Y. Zhao, "Tactic to improve detecting accuracy on robotic system with structural installation error," in *Proc. IEEE 4th Inf. Technol., Netw., Electron. Automat. Control Conf. (ITNEC)*, Jun. 2020, pp. 1880–1883.

[7] T. Messay, R. Ordóñez, and E. Marcil, "Computationally efficient and robust kinematic calibration methodologies and their application to industrial robots," *Robot. Comput.-Integr. Manuf.*, vol. 37, pp. 33–48, Feb. 2016.

[8] G. B. Gao, G. Q. Sun, J. Na, Y. Guo, and X. Wu, "Structural parameter identification for 6 DOF industrial robots," *Mech. Syst. Signal Process.*, vol. 113, pp. 145–155, Dec. 2018.

[9] T. Chen, J. Lin, D. Wu, and H. Wu, "Research of calibration method for industrial robot based on error model of position," *Appl. Sci.*, vol. 11, no. 3, p. 1287, Jan. 2021.

[10] H. X. Nguyen, H. Q. Cao, T. T. Nguyen, T. N.-C. Tran, H. N. Tran, and J. W. Jeon, "Improving robot precision positioning using a neural network based on Levenberg Marquardt–APSO algorithm," *IEEE Access*, vol. 9, pp. 75415–75425, 2021.

[11] H. Q. Cao, H. X. Nguyen, T. T. Nguyen, V. Q. Nguyen, and J. W. Jeon, "Robot calibration method based on extended Kalman filter-dual quantum behaved particle swarm optimization and adaptive neuro-fuzzy inference system," *IEEE Access*, vol. 9, pp. 132558–132568, 2021.

[12] S. Diao, X. Chen, and L. Wu, "Calibration method of vision measurement system for ceramic billet grinding robot," *J. Eng.*, vol. 2019, no. 7, pp. 4656–4666, Jul. 2019.

[13] A. Nubiola and I. A. Bonev, "Absolute calibration of an ABB IRB 1600 robot using a laser tracker," *Robot. Comput.-Integr. Manuf.*, vol. 29, no. 1, pp. 236–245, Feb. 2013.

[14] A. Nubiola and I. A. Bonev, "Absolute robot calibration with a single telescoping ballbar," *Precis. Eng.-J. Int. Soc. Precis. Eng. Nanotechnol.*, vol. 38, no. 3, pp. 472–480, Jul. 2014.

[15] J. Santolaria, J. Conte, and M. Ginés, "Laser tracker-based kinematic parameter calibration of industrial robots by improved CPA method and active retroreflector," *Int. J. Adv. Manuf. Technol.*, vol. 66, nos. 9–12, pp. 2087–2106, Jun. 2013.

[16] M. Gaudreault, A. Joubair, and I. Bonev, "Self-calibration of an industrial robot using a novel affordable 3D measuring device," *Sensors*, vol. 18, no. 10, p. 3380, Oct. 2018.

[17] S. Hu, M. Zhang, C. Zhou, and F. Tian, "A novel self-calibration method with POE-based model and distance error measurement for serial manipulators," *J. Mech. Sci. Technol.*, vol. 31, no. 10, pp. 4911–4923, Oct. 2017.

[18] Q. Zhu, X. Xie, C. Li, G. Xia, and Q. Liu, "Kinematic self-calibration method for dual-manipulators based on optical axis constraint," *IEEE Access*, vol. 7, pp. 7768–7782, 2019.

[19] C. Icli, O. Stepanenko, and I. Bonev, "New method and portable measurement device for the calibration of industrial robots," *Sensors*, vol. 20, no. 20, p. 5919, Oct. 2020.

[20] J. Shi, H. Zhang, Y. Liu, D. Wang, and L. Gao, "A self-calibration method for robot based on geometric constraints," in *Proc. IEEE Int. Conf. Inf. Automat. (ICIA)*, Aug. 2016, pp. 1863–1867.

[21] S. He, L. Ma, C. Yan, C.-H. Lee, and P. Hu, "Multiple location constraints based industrial robot kinematic parameter calibration and accuracy assessment," *Int. J. Adv. Manuf. Technol.*, vol. 102, nos. 5–8, pp. 1037–1050, Jun. 2019.

[22] A. Joubair and I. A. Bonev, "Kinematic calibration of a six-axis serial robot using distance and sphere constraints," *Int. J. Adv. Manuf. Technol.*, vol. 77, nos. 1–4, pp. 515–523, Mar. 2015.

[23] R. Wang, G. Yang, H. Zhao, and J. Luo, "Robot kinematic calibration with plane constraints based on POE formula," in *Proc. IEEE Int. Conf. Inf. Automat. (ICIA)*, Aug. 2016, pp. 1887–1892.

[24] E. Nieves, N. Xi, B. Q. Du, and Y. Y. Jia, "A reflected laser line approach for industrial robot calibration," in *Proc. IEEE Int. Conf. Adv. Intell. Mechatronics*, Jul. 2012, pp. 610–615.

[25] B. Gao, Y. Liu, N. Xi, and Y. Shen, "Developing an efficient calibration system for joint offset of industrial robots," *J. Appl. Math.*, vol. 2014, pp. 1–9, Jan. 2014.

[26] S. Du, J. Ding, and Y. Liu, "Industrial robot kinematic calibration using virtual line-based sphere surface constraint approach," in *Proc. IEEE Int. Conf. Cyber Technol. Automat., Control, Intell. Syst. (CYBER)*, Jun. 2015, pp. 48–53.

[27] Y. Guo, B. Song, X. Tang, X. Zhou, Y. Xie, and J. Jin, "Calibration for kinematic parameters of industrial robot by a laser displacement sensor," in *Proc. 15th Int. Conf. Control, Automat., Robot. Vis. (ICARCV)*, Nov. 2018, pp. 1829–1833.

[28] *Metrology Terminology Approval Committee, Chinese Terms in Metrology*, Sci. Press, China, 2015.

XIRUI LI received the bachelor's degree from the Hefei University of Technology, Hefei, China, in 2019. He is currently pursuing the master's degree with the Faculty of Mechanical Engineering & Automation, Zhejiang Sci-Tech University, Hangzhou, China. His research interests include robot calibration and motion control.

XIUJUN FANG received the bachelor's degree from Shanxi Agricultural University, Jinzhong, China, in 2020. He is currently pursuing the master's degree with the Faculty of Mechanical Engineering & Automation, Zhejiang Sci-Tech University, Hangzhou, China. His research interests include robotics and vision guidance for robot assembly.

ENZHENG ZHANG received the Ph.D. degree from the Beijing Institute of Technology, Beijing, China, in 2015. He is currently a Teacher in the measuring and controlling technology and instrument specialty of mechanical engineering and automation with Zhejiang Sci-Tech University, Hangzhou, China. His research interests include robot skills learning and intelligent manufacturing.

BIN ZHAI received the bachelor's degree from Zhejiang Sci-Tech University, Hangzhou, China, in 2020. He is currently pursuing the master's degree with the Faculty of Mechanical Engineering & Automation, Zhejiang Sci-Tech University. His research interests include robotics and control theory.